The exported chaperone PfHsp70x is dispensable for the *Plasmodium falciparum* intraerythrocytic lifecycle.

David W. Cobb*[1,2], Anat Florentin*[1,2], Michelle Krakowiak[1,2], Vasant Muralidharan[#,1,2]

[1] Department of Cellular Biology

[2] Center for Tropical and Emerging Global Diseases

University of Georgia, Athens, Georgia, United States of America

*These authors contributed equally to this work.

[#] Corresponding author: vasant@uga.edu

Abstract

Export of parasite proteins into the host erythrocyte is essential for survival of *Plasmodium falciparum* during its asexual lifecycle. While several studies described key factors within the parasite that are involved in protein export, the mechanisms employed to traffic exported proteins within the host cell are currently unknown. Members of the Hsp70 family of chaperones, together with their Hsp40 co-chaperones, facilitate protein trafficking in other organisms, and are thus likely used by *P. falciparum* in the trafficking of its exported proteins. A large group of Hsp40 proteins is encoded by the parasite and exported to the host cell, but only one Hsp70, PfHsp70x, is exported with them. PfHsp70x is absent from most *Plasmodium* species and is found only in *P. falciparum* and closely-related species that infect Apes. Herein, we have utilized CRISPR/Cas9 genome editing in *P. falciparum* to investigate the essentiality of PfHsp70x. We show that parasitic growth was unaffected by knockdown of PfHsp70x using both the DHFR-based Destabilization Domain and the *glmS* ribozyme system. Similarly, a complete gene knockout of PfHsp70x did not affect the ability of *P. falciparum* to proceed through its intraerythrocytic lifecycle. The effect of PfHsp70x knockout on the export of proteins to the host RBC was tested and we found that this process was unaffected. These data show that although PfHsp70x is the sole exported Hsp70, it is not essential for the asexual development of *P. falciparum*.

Introduction

Malaria is a profound killer worldwide. In 2015, 214 million cases of malaria resulted in 438,000 deaths, largely in Africa and Asia [1]. Within malaria endemic countries, the

disease targets the most vulnerable of the population, including children under five and pregnant women [1]. The disease is caused by infection with eukaryotic parasites from the genus *Plasmodium*, but it is one species—*P. falciparum*—that is responsible for most of the malaria associated mortality. The clinical manifestations of malaria range from fever, headache, and muscle pains, to severe anemia, coma, and respiratory distress [2]. All of these symptoms are direct consequences of asexual replication of the parasite within the human red blood cell (RBC)[3]. During this cycle of replication, *P. falciparum* invades the RBC and dramatically transforms its morphology and physiology. Alterations to the RBC include increased permeability, loss of cell deformability, and introduction of virulence-associated knobs at the RBC membrane [4,5].

Remodeling of the RBC requires export of hundreds of parasite proteins into the host cell, a feat involving protein trafficking through multiple compartments before arriving at their final destinations in the host. The first phase of the journey begins in the parasite endoplasmic reticulum (ER). Many exported proteins contain an N-terminal signal motif termed the Host Targeting Signal or *Plasmodium* Export Element (PEXEL) (6, 7). A key step in the export of PEXEL-containing proteins is cleavage of the motif by the ER-resident aspartyl protease Plasmepsin V (PMV) (8–10). A sub-group of exported proteins called PEXEL-Negative Exported Proteins (PNEPs) lack the motif, but their N-terminus is similarily necessary for export [11,12]. Aside from Plasmepsin V processing of PEXEL, mechanisms underlying the selection of host-destined proteins for exit from the ER remain unclear. Nonetheless, PEXEL-proteins and PNEPs continue their journey through the parasite's secretory pathway and are delivered to the

parasitophorous vacuole (PV), a membranous structure within which the parasite resides. Previous studies have shown that proteins cross the parasitophorous vacuole membrane (PVM) through the *Plasmodium* Translocon of Exported Proteins (PTEX) [13–15] . Once they are on the other side of the PVM, all classes of proteins need to refold and find their specific subcellular localization, whether it is in the host cytoplasm, the host membrane, or parasite-induced structures such as knobs or Maurer's clefts. It is completely unknown how hundreds of proteins, within a short time period, cross through PTEX, refold to regain structure and function, and find their final destination in the host.

The process of protein export is essential for *P. falciparum* survival in the RBC, as blockage of protein export—whether at the parasite ER or at the PVM—results in parasite death. In the ER, overexpression of catalytically dead PMV results in impaired parasite growth, and inhibition of PMV with a PEXEL-mimetic impairs protein export and kills parasites during the transition to the trophozoite stage [9,16,17]. Similarly, *P. falciparum* parasites are sensitive to interference of trafficking across the PVM. Conditional knockdown of PTEX components blocks protein export and kills the parasites [18,19]. As the parasites are susceptible to inhibition of trafficking in the ER and PV, interference in the trafficking process within the host may similarly impair parasite growth. The mechanisms of protein trafficking inside of the host cell remain unknown, but identification of essential components of this process will provide valuable targets for drug discovery programs.

Molecular chaperones are likely candidates in the search for key export and trafficking components. Indeed, PfHsp101 is an essential component of PTEX, and its inhibition results in accumulation of exported proteins within the PV [18]. Furthermore, several parasite Hsp40s are exported to the RBC, but their function there is unknown [20]. In other organisms Hsp40s serve as co-chaperones for Hsp70s, but in contrast to the large number of exported Hsp40s, PfHsp70x (PF3D7_0831700) is the only parasite-encoded Hsp70 that is exported to host cell [21,22]. This chaperone is found in *P. falciparum* and *P. reichenowi*, but not in other *Plasmodium* species that infect humans, such as *P. vivax* or *P. knowlesi* [21]. Within the *P. falciparum* infected RBC, PfHsp70x is localized to the PV and the host, where it associates with PfHsp40s in mobile structures termed J-dots [21]. Given its status as sole exported Hsp70, we hypothesized that PfHsp70x is central to protein trafficking in the host cell, and thus essential to parasite viability. Indeed, studies focused on PTEX interactions have found PfHsp70x associated with the translocon, and it has been shown to co-localize with virulence proteins during their trafficking [21,23,24].

In this study, we took advantage of various genetic tecniques to show that PfHsp70x is non-essential for protein export and parasite growth. We have used the DHFR-based destabilizing domain that has previously been used to inhibit chaperone function [18,25]. In addition, we have used the *glmS*-ribozyme system that inhibits translation via mRNA degradation [26]. Mutants were successfully generated for each system, but knockdown had no impact on protein export or parasite growth. To confirm that the lack of a phenotype was not due to incomplete knockdown, we used CRISPR/Cas9

technology to generate a complete knockout of the PfHsp70x gene and found no defects in parasite proliferation. Our data demonstrate that PfHsp70x is not required for protein export to the host RBC and is not essential for the intraerythrocytic lifecycle of *P. falciparum*.

Results and Discussion

Conditional inhibition of PfHsp70x activity using the DHFR-based Destabilization Domain. Previous work has shown that chaperones fused to a DHFR-based destabilization domain (DDD) are auto-inhibited when the DDD is in its unfolded state [18,25], unlike other proteins which are degraded when fused to the DDD [27–29]. In the presence of the stabilizing ligand trimethoprim (TMP), the DDD is folded and the chaperone functions normally. However, upon TMP removal the DDD is unfolded and binds to its attached chaperone intramolecularly, thereby blocking interactions with the chaperone's client proteins and inhibiting normal chaperone function (**Fig. 1A**). Relying on a single-crossover homologous recombination, the *pfhsp70x* gene was modified with a triple-HA tag and the DDD, and integration at the *pfhsp70x* locus was confirmed via Southern blot analysis (**Fig. 1A, B**). Consistent with the auto-inhibitory model of chaperone-DDD action, western blot analysis of parasite lysates following TMP removal showed that PfHsp70x protein levels remain consistent over time (**Fig. 1C**). Isolation of the host cell cytoplasm using saponin lysis revealed that PfHsp70x-DDD is exported to the host cell. Moreover, the persistence of PfHsp70x in the supernatant following TMP removal indicated that PfHsp70x is exported to the host cell even in its putative inhibited form. To assess the role of PfHsp70x in parasite proliferation, we removed TMP and

measured asexual growth over a course of several days and at least two replication cycles. We found that the absence of TMP had no effect on parasite proliferation (**Fig. 2A**). It was previously reported that PfHsp70x , together with several other exported chaperones, localizes to specific punctate structures in the host cell termed J-dots. To test the effect of DDD-based inhibition on PfHsp70x localization, we performed immunofluorescence assays and found that PfHsp70x-DDD is trafficked to the expected punctate structures within the host cell, regardless of TMP presence (**Fig. 2B**). These data suggest that inhibition of PfHsp70x activity using the DDD system does not affect the asexual life cycle of the parasite. Nevertheless, we could not assess the degree of inhibition and therefore could not exclude the possibility that the chaperone activity was unaffected by the DDD fusion, leading to the lack of a growth phenotype. We therefore utilized alternative methods to reduce PfHsp70x protein levels in the parasite.

Fig. 1. Generating PfHsp70x-DDD parasites. (A) Mechanism of PfHsp70x-DDD conditional inhibition. The *pfhsp70x* locus was modified to contain a triple hemagglutinin (HA) tag and a DHFR-based destabilization domain (DDD). In the presence of trimethoprim (TMP) the DDD is stable and the chaperone is active. Upon TMP removal the chaperone binds the DDD intra-molecularly and cannot interact with client proteins, inhibiting normal activity. (B) Single crossover homologous recombination enables the integration of the plasmid into the 3’ end of the *pfhsp70x* gene (upper panel). Southern blot analysis of genomic DNA (bottom panel) isolated from parasite lines indicated above the lanes. The genomic DNA was digested with AccI. Bands expected from integration of the plasmid into the 3’ end of the *pfhsp70x* gene were observed in two

independent transfections. A single band indicative of the parental allele was observed for the parental strain and it was absent in the integrant parasites. (C) PfHsp70x-DDD parasites were incubated without TMP, and Schizont stage parasites were purified on a percoll gradient. Host cell lysates together with exported proteins were isolated using 0.04% cold saponin and were then collected from the supernatant (S). Parasites cells with all non-exported proteins were collected from the pellet (P). Using western blot analysis, the two fractions were analyzed and probed for PfHsp70x expression and export. The membrane was probed with antibodies against HA (top) and Plasmepsin V (loading control, bottom). The protein marker sizes that co-migrated with the probed protein are shown on the left.

Fig. 2. TMP removal does not affect parasite growth and PfHsp70x localization. (A) Asynchronous PfHsp70x-DDD parasites were grown with or without 10µM TMP and parasitemia was monitored every 24 hours over 5 days. Data are fit to an exponential growth equation and are represented as mean ± S.E.M. Experiments were done 3 times and biological replicates are shown. (B) Immunofluorescence imaging of acetone fixed PfHsp70x-DDD parasites stained with antibodies against HA (green) and DAPI (blue). Scale bar, 5µm.

Conditional Knockdown of PfHsp70x Using the *glmS* Ribozyme. Next, we sought to conditionally knockdown PfHsp70x at the mRNA level using the *glmS* ribozyme [26]. In this system, the *glmS* ribozyme sequence is inserted into the 3' end of the genomic locus of a gene and is transcribed with the gene as one mRNA. Addition of the small

molecule glucosamine (GlcN) activates the *glmS* ribozyme, which cleaves itself from the mRNA, disconnecting the transcript form its polyA tail and leading to its degradation (**Fig. 3A**). Using CRISPR/Cas9 genome engineering, we appended a triple HA tag to the C-terminus of PfHsp70x followed by the *glmS* ribozyme (**Fig. 3A**) [30]. A second cell line was generated in which the *pfhsp70x* locus was tagged with a mutant version of the ribozyme—termed *M9*—which is unresponsive to GlcN and serves as a control during GlcN treatment. Following transfection and drug selection, PfHsp70x-*glmS* and PfHsp70x-*M9* clones were isolated via limiting dilution. PCR analysis revealed the correct integration of the tag and ribozyme into the *pfhsp70x* gene in all clonal parasite lines (**Fig. 3B**). Additionally, immunofluorescence assays confirmed that PfHsp70x-*glmS* is exported to the host cytoplasm, where it is found, as before, in punctate structures that are distinct from Maurer's clefts, suggestive of J-dot localization (**Fig. 3C**).

Fig. 3. CRISPR/Cas9-mediated integration of HA-*glmS*/*M9* at PfHsp70x locus. (A) Diagram showing integration of 3xHA-ribozyme sequence and GlcN-induced degradation of mRNA. Cas9 introduces a double-stranded break at the beginning of the 3' UTR of the *pfhsp70x* locus. The repair plasmid provides homology regions for double-crossover homologous recombination, introducing a 3xHA tag and the ribozyme sequence. Following translation and addition of GlcN, the PfHsp70x-*glmS* mRNA is cleaved by the ribozyme and is subject to degradation. (B) PCR test confirming integration at the PfHsp70x locus. DNA was purified from transfected, cloned parasites and primers were used to amplify the region between the C-terminus and 3'UTR of

pfhsp70x. The PCR products were digested with AfeI, further confirming integration. (C) IFA showing export of HA-tagged PfHsp70x. Asynchronous PfHsp70x-*glmS* parasites were fixed with acetone and stained with specific antibodies. Images from left to right are phase, DAPI (parasite nucleus, blue), anti-HA (red), anti-MAHRP1 (green), and fluorescence merge. Scale bar represents 5 µm. (R) ring, (T) trophozoite, and (S) schizont.

We tested the effect of reducing PfHsp70x expression on intraerythrocytic growth. To ensure that insertion of the ribozyme itself does not interfere with normal asexual growth, PfHsp70x-*glmS*, PfHsp70x-*M9*, and the parental line (3D7) were grown in the absence of GlcN. Indeed, we found that in the absence of GlcN, growth of both the *glmS* and *M9* cell lines was comparable to 3D7 (**Fig. 4A**). Next, PfHsp70x-*glmS* and PfHsp70x-*M9* were cultured with GlcN and parasitemia was measured via flow cytometry. The growth of PfHsp70x-*glmS* and PfHsp70x-*M9* was unaffected by treatment with 5 mM and 10 mM GlcN (**Fig. 4B, C**). To confirm that PfHsp70x protein level is reduced in response to GlcN, schizont-stage parasites from the *glmS* and *M9* cell lines were Percoll-purified and whole parasite lysates were used for Western blotting. Using anti-HA antibody we found that treatment with GlcN reduced protein levels in PfHsp70x-*glmS* but did not affect protein levels in PfHsp70x-*M9* (**Fig. 4D**). Together, these data show that we can efficiently reduce PfHsp70x levels using the *glmS* ribozyme but this has no affect on the asexual growth of the parasite within the RBC.

Fig. 4. GlcN-induced knockdown of PfHsp70x does not affect intraerythrocytic growth. (A) PfHsp70x-*glmS*, PfHsp70x-*M9*, and 3D7 (parental line) were seeded at equal parasitemia in triplicate and grown in normal culturing media (complete RPMI). Parasitemia was measured every 24 hours using flow cytometry. Data are fit to an exponential growth equation and are represented as mean ± S.E.M. (n=3). (B) and (C) PfHsp70x-*glmS* and PfHsp70x-*M9* parasites were seeded at equal parasitemia in triplicate. Cultures were grown in the presence of either 5 mM (B) or 10 mM (C) GlcN. Parasitemia was measured every 24 hours using flow cytometry. Data are fit to an exponential growth equation and are represented as mean ± S.E.M. (n=3). (D) PfHsp70x-*glmS* and PfHsp70x-*M9* parasites were grown in the presence of 7.5 mM GlcN. Schizont-stage parasites were Percoll-purified every 24 hours, and whole parasite lysates were used for western blot analysis. Membrane was probed with anti-HA, and anti-PfEF1α (loading control).

Protein export is unimpaired in PfHsp70x-knockdown parasites. Although parasite growth was unaffected by PfHsp70x knockdown, we reasoned that it could nonetheless play a role in export of proteins to the host cell. In particular, we hypothesized that PfHsp70x is needed for the export of proteins known to mediate virulence of *P. falciparum* infection, as trafficking defects of these proteins would not manifest as arrest of the asexual lifecycle [20]. Using immunofluorescence, we examined localization of specific virulence-associated proteins in PfHsp70x-*M9* and PfHsp70x-*glmS* parasites after 72 hours of growth in GlcN-supplemented media. First, the localization of the PEXEL-containing PfFIKK4.2, an exported kinase associated with knob formation and

infected RBC rigidity [31], is unchanged in control versus PfHsp70x-knockdown parasites **(Fig. 5A)**. Next, we examined the localization of the PEXEL-containing protein KAHRP, which is essential for the formation of knobs on the surface of infected RBCs [32]. Export of this protein was not inhibited in PfHsp70x-knockdown parasites **(Fig. 5B)**. Finally, we determined the localization of the PNEP MAHRP1, which has been implicated in the presentation of antigenically variant proteins at the RBC surface [33], and found that its export is not impaired by the knockdown of PfHsp70x **(Fig. 5C)**. As demonstrated by HA-staining in western blot and IFA (**Fig. 4D**, **Fig. 5**), PfHsp70x is reduced, but not completely ablated, using the *glmS* ribozyme. We reasoned that the reduced level of PfHsp70x that is produced during GlcN treatment could be sufficient for parasite survival, and therefore endeavored next to knockout *pfhsp70x*.

Fig. 5. PfHsp70x knockdown does not inhibit export of virulence-associated proteins. Asynchronous PfHsp70x-HA-*M9* PfHsp70x-*glmS* parasites were fixed with acetone (PfFIKK4.2 and MAHRP1) or paraformaldehyde (KAHRP) and stained with antibodies against (A) PfFIKK4.2, (B) KAHRP, and (C) MAHRP1. DAPI used to mark parasite cell nucleus. Scale bar represents 5µm. Images from left to right are phase, DAPI (blue), anti-exported protein (green), anti-HA (red), and fluorescence and phase merge. Representative images shown.

Knockout of *pfhsp70x* does not affect parasite growth*.* We successfully utilized two different conditional knockdown approaches to modify PfHsp70x activity and expression, but these knockdowns were insufficient to produce a growth or protein

export defect in the parasites. Therefore, we sought to definitively test the essentiality of PfHsp70x via complete genomic knockout (termed PfHsp70x-KO). To this end, we employed CRISPR/Cas9 to interrupt the PfHsp70x ORF by inserting a human dihydrofolate reductase (*hdhfr*) drug resistance cassette (**Fig. 6A**). Following transfection and selection with WR99210, PfHsp70x-KO parasites were cloned via limiting dilution. Southern blot analysis of genomic DNA isolated from the parental line and independent clones showed that the *hdhfr* cassette was inserted into the *pfhsp70x* gene via homology directed repair (**Fig. 6B**). To verify that the null mutants do not express PfHsp70x, schizont-stage parasites from two independent knockout clones and the parental line were Percoll-purified, and whole parasite lysates were used for Western blotting. Probing with anti-PfHsp70x shows that the knockout clones do not express PfHsp70x (**Fig. 6C**). Finally, intraerythrocytic growth of the PfHsp70x-KO clones was monitored over two replication cycles. In agreement with the lack of any growth phenotype in the conditional knockdown parasite lines, the PfHsp70x-KO parasites displayed *wild-type* level of proliferation in erythrocytes (**Fig. 6D**). The normal growth in the complete absence of PfHsp70x expression conclusively demonstrates that PfHsp70x activity is not essential for the asexual growth of the parasite within the RBC in culture.

Fig. 6. Knockout of *pfhsp70x* does not affect intraerythrocytic growth. (A) Schematic showing interruption of PfHsp70x ORF with *hDHFR* cassette. Cas9-mediated double-stranded break in the *pfhsp70x* ORF is repaired using homology regions on the template plasmid while inserting an *hDHFR* cassette into the locus. (B)

Southern blot analysis confirming knockout of PfHsp70x. Genomic DNA from independent knockout clones (A3, A7, B3, and B9) was isolated and digested with BamHI and ScaI. Membrane was hybridized with a biotin-labeled probe complementary to the first 800 base pairs of the *pfhsp70x* gene. (C) Western blot analysis demonstrating loss of PfHsp70x protein expression in independent knockout clones. Schizont-stage parasites were Percoll-purified, and whole cell lysate was used for analysis. Membrane was probed with antibodies raised against PfHsp70x, and against Plasmepsin V as a loading control. (D) Parental line and independent PfHsp70x-KO clones (A7 and B3) were seeded at equal parasitemia in triplicate. Parasitemia was measured every 24 hours using flow cytometry. Data are fit to an exponential growth equation and are represented as mean ± S.E.M. (n=3).

Protein export is unimpaired in PfHsp70x-KO parasites. In order to confirm that the successful export of proteins in the PfHsp70x-knockdown parasites was not due to the residual PfHsp70x produced during GlcN treatment, we examined the localization of the same exported proteins in the PfHsp70x-KO parasites. We found that the virulence proteins PfFIKK4.2, KAHRP, and MAHRP are successfully exported to the host cell despite the complete absence of PfHsp70x (**Fig. 7A-C**). These data support the results from the PfHsp70x knockdown and show that loss of PfHsp70x does not impede the parasite's ability to export virulence-associated proteins to the host cell.

Fig. 7. PfHsp70x knockout does not inhibit export of virulence-associated proteins. Asynchronous 3D7 and PfHsp70x-KO parasites were fixed with acetone

(PfFIKK4.2 and MAHRP1) or paraformaldehyde (KAHRP) and stained with antibodies against (A) PfFIKK4.2, (B) KAHRP, and (C) MAHRP1. DAPI used to mark parasite cell nucleus. Scale bar represents 5µm. Images from left to right are phase, DAPI (blue), anti-exported protein (green), and fluorescence and phase merge. Representative images shown.

Even though PfHsp70x is the only parasite-encoded Hsp70 that is exported to the RBC, our results demonstrate that it is not required for intraerythrocytic growth. However, PfHsp70x is not the only Hsp70 found in infected RBCs. Human Hsp70 is present in the erythrocyte cytoplasm [34]. Thus, the role played by PfHsp70x in the parasite's biology could be redundant with the human Hsp70 that is already present in the host cell. In fact, infection with *P. falciparum* affects the normal localization of the human Hsp70, as the protein is soluble in non-parasitized RBCs but is found in detergent-resistant fractions following infection [35]. The methods used here to investigate the function of PfHsp70x, knockdown and complete genomic knockout, are more challenging to use for human Hsp70. The mature RBC cannot be genetically manipulated, and knockdown of human Hsp70 in hematopoietic stem cells abrogates RBC formation [36]. Furthermore, detailed analysis of the *pfhsp70x* locus in strains isolated from the field may be informative about the essentiality of PfHsp70x in human infections. Overall, our data demonstrate that PfHsp70x is not required for export of *P. falciparum* effector proteins to the host and is dispensible for asexual growth within human RBCs.

Materials and Methods

Plasmid construction. Genomic DNA was isolated from *P. falciparum* using the QIAamp DNA blood kit (QIAGEN). Constructs utilized in this study were confirmed by sequencing. PCR products were inserted into the respective plasmids using the In-Fusion cloning system (Clonetech) or using the sequence and ligation independent cloning method. Briefly, insert and cut vector were mixed with a T4 DNA polymerase and incubated for 2.5 minutes at room temperature, followed by 10 minutes incubation on ice and then transformed into bacteria. For generation of plasmid PfHsp70x-HADB, a 1-kb homologous sequence from the 3'-end of the *pfhsp70x* gene (not including the stop codon) was amplified by PCR using primers 5'-CACTATAGAACTCGAGGTGAAAAAGCTAAACGTGTATTATCATCATCCGCACAAGC-3' and 5'-CGTATGGGTACCTAGGATTTACTTCTTCAACGGTTGGTCCATTATTTTGTGC-3' and was inserted into pHADB (18) using restriction sites XhoI and AvrII (New England Biolabs).

For the generation of the *glmS* conditional mutants three plasmids were used; 1) pUF1-Cas9 (from J. J. Lopez-Rubio) was used to drive cas9 expression [30]. 2) pMK-U6 was used to drive expression of the RNA guide. For this purpose, pL6 plasmid (from J. J. Lopez-Rubio, [30]) was digested with NotI and NcoI (New England Biolabs) and the fragment that contained the U6 RNA expression cassette was blunted and re-ligated to form the pMK-U6 plasmid. The guideRNA, oligos 5'-TAAGTATATAATATTTGCATTATTGTTGTATATTTGTTTTAGAGCTAGAA-3' and 5'-TTCTAGCTCTAAAACAAATATACAACAATAATGCAAATATTATATACTTA-3' were

annealed and cloned into the RNA module in MK-U6 as previously described [30]. Briefly, pMK-U6 was digested with BtgZI (New England Biolabs) and annealed oligos were inserted using In-Fusion HD Cloning Kit (Clontech). 3) pHA-glmS and pHA-M9 were used as donor DNA templates consisting of two homology regions flanking the HA tag and the *glmS* (or the *M9*) sequences. To generate the pHA-glmS and pHA-M9 plasmids, primers 5'-GAGCTCGCTAGCAAGCTTGCCGGCAAGATCATGTGATTTCTCTTTGTTCAAGGAGTC-3' and 5'-TCCGCGGAGCGCTACTAGTTACCCATACGATGTTCCAGATTACGCTTACCCATACGATGTTCCAGATTACGCTTACCCATACGATGTTCCAGATTACGCTTAAATGTCCAGACCTGCAGTAATTATCCCGCCCGAACTAAGCGC-3' were used to amplify the *glmS* and *M9* sequences from pGFP-glmS and pGFP-M9, respectively (from P.Shaw, [26]). PCR constructs were then inserted into a TOPO cloning vector (ThermoFisher). To allow efficient genomic integration of the pHA-glmS and pHA-M9 donor plasmids, 800bp sequences were used for each homology region. The C-terminus of the *pfhsp70x* coding region was PCR amplified form genomic DNA using primers 5'-AATTCGCCCTTCCGCGGGCTGTACAAGCAGCCATCTTATCAGGTGATCAATCATC-3' and 5'-ATCGTATGGGTAAGCGCTATTTACTTCTTCAACGGTTGGTCCATTATTTTGTGCTTC-3' and was inserted into pHA-glmS and pHA-M9 using restriction sites SacII and AfeI (New England Biolabs). The 3'UTR of *pfhsp70x* was pcr amplified from genomic DNA using primers 5'-ATGATCTTGCCGGCAAGCTTACGAAAATATACAACAATAATGCATAAAATAATAATA

ATT-3’ and 5’-
CCTTGAGCTCGCTAGCGCAATATAAATGGATTATTCCTTTTGTATATAATTTAAAATA
AG-3’ and was inserted into pHA-glmS and pHA-M9 (already containing the C-terminus homology region) using restriction sites HindIII and NheI (New England Biolabs).
For the generation of *pfhsp70x-ko* parasites two plasmids were used; 1) A cas9 expressing plasmid (as described above), and 2) pL7-PfHsp70x plasmid that is derived from the pL6 plasmid (from J. J. Lopez-Rubio, [30]). pL7-PfHsp70x contained the guide RNA and 800bp homology regions flanking a *hdhfr* gene that confers resistance to WR. The N-terminus of the *pfhsp70x* gene was amplified via PCR from genomic DNA using primers 5’- cggggaggactagtATGAAGACAAAAATTTGTAGTTATATTCATTATATTG-3’ and 5’- acaaaatgcttaagGGAAACATCTTTACCTCCATTTTTTTTTTTAAAATCTTGTAC-3’ and was inserted into pL6 using restriction sites AflII and SpeI (New England Biolabs). The C-terminus of the *pfhsp70x* gene was pcr amplified from genomic DNA using primers 5’-
taaatctagaattcTGATCAATCATCAGCTGTCAAAGACTTATTATTATTAGATG-3’ and 5’-
ttaccgttccatggTTAATTTACTTCTTCAACGGTTGGTCCATTATTTTGTGCTTC-3’ and was inserted into pL6 (already containing the C-terminus homology region) using restriction sites NcoI and EcoRI (New England Biolabs). In order to insert the guide DNA sequence, oligos 5’-
TAAGTATATAATATTGTACAAGCAGCCATCTTATCGTTTTAGAGCTAGAA-3’ and 5’-
TTCTAGCTCTAAAACGATAAGATGGCTGCTTGTACAATATTATATACTTA-3’ were annealed and cloned into pL6 as previously described [30]. Briefly, pL6 was digested

with BtgZI (New England Biolabs) and annealed oligos were inserted using In-Fusion HD Cloning Kit (Clontech).

Cell culture and transfections. Parasites were cultured in RPMI medium supplemented with Albumax I (Gibco) and transfected as described earlier [37,38]. For generation of *PfHsp70x-DDD* parasites, PfHsp70x-HADB was transfected in duplicates into 3D7-derived parental strain PM1KO which contains a *hDHFR* expression cassette conferring resistance to TMP [39]. Selection and drug cycling were performed as described [25] in the presence of 10 μM of TMP (Sigma). Integration was detected after three rounds of drug cycling with blasticidin (Sigma).

For generation of PfHsp70x-*glmS* and PfHsp70x-*M9* parasites, a mix of three plasmids (40 µg of each) was transfected in duplicates into 3D7 parasites. The plasmids mix contained pUF1-Cas9 (from J. J. Lopez-Rubio, [30]) which contains the *DHOD* resistance gene, pMK-U6-PfHsp70x, pHA-glmS-PfHsp70x or pHA-M9-PfHsp70x, which are all marker-free. Drug pressure was applied 48 hours post transfection, using 1μM DSM [40], selecting only for Cas9 expression. Drug was removed from the culturing media once parasites became detectable in the culture, usually around 3 weeks post transfection.

For generation of PfHsp70x-KO parasites, a mix of pUF1-Cas9 (from J. J. Lopez-Rubio, [30]) and pL7-PfHsp70x (50 µg of each plasmid) was transfected in duplicates into 3D7 parasites. Drug pressure was applied 48 hours post transfection, using 2.5nM

427 WR99210 (Sigma), selecting for integration of the drug resistance cassette into the
428 *pfhsp70x* gene.
429
430 **Growth assays.** For asynchronous growth assays of PfHsp70x-DDD lines, parasites
431 were washed twice and incubated without TMP. For asynchronous growth assays of
432 PfHsp70x-*glmS* and PfHsp70x-*M9 parasites*, 5 or 10 mM GlcN (Sigma) were added to
433 the growth media. Asynchronous growth assays of PfHsp70x-KO parasites were
434 performed in media containing WR99210. Parasitemia was monitored every 24 hours
435 via flow cytometry. For flow cytometry, aliquots of parasite cultures (5 μl) were stained
436 with 1.5 mg/ml Acridine Orange (Molecular Probes) in PBS. The fluorescence profiles of
437 infected erythrocytes were measured by flow cytometry on a CyAn ADP (Beckman
438 Coulter) or CytoFLEX (Beckman Coulter) and analyzed by FlowJo software (Treestar,
439 Inc.). Whenever required, parasites were sub-cultured to avoid high parasite density
440 and relative parasitemia at each time point was back-calculated based on actual
441 parasitemia multiplied by the relevant dilution factors. 100% parasitemia was
442 determined as the highest relative parasitemia and was used to normalize parasite
443 growth. Data were fit to exponential growth equations using Prism (GraphPad Software,
444 Inc.)
445
446 **Southern blotting.** Southern blots were performed with genomic DNA isolated using
447 the Qiagen Blood and Cell Culture kit. 10 μg of DNA was digested overnight with
448 NcoI/XmnI for PfHsp70x-DDD and BamHI/ScaI for PfHsp70x-KO (New England
449 Biolabs). Integrants were screened using biotin-labeled probes against the 3'-end

(PfHsp70x-DDD parasites) or 5'-end (PfHsp70x-KO parasites) of the *pfhsp70x* gene. Southern blot was performed as described earlier [41]. The probe was labeled using biotinylated Biotin-16-dUTP (Sigma). The biotinylated probe was detected on blots using IRDye 800CW dye conjugated to Streptavidin (LICOR Biosciences) and was imaged, processed and analyzed using the Odyssey infrared imaging system software (LICOR Biosciences).

Western blotting. Western blots were performed as described previously [27]. Briefly, late-stage parasites were isolated on a percoll gradient (Genesee Scientific). For PfHsp70x-DDD parasites, host RBCs were permeabilized selectively by treatment with ice-cold 0.04% saponin in PBS for 10 min. Supernatants were collected for detection of exported parasites proteins and pellets were collected for detection of proteins with the parasite. For PfHsp70x-KO, PfHsp70x-*glmS* and PfHsp70x-*M9* parasites, whole parasite lysates, including the host RBC, were used to detect protein expression and export. The antibodies used in this study were rat anti-HA (3F10, Roche, 1:3000), rabbit anti-PfEF1α (from D. Goldberg, 1: 2000), mouse anti-Plasmepsin V (From D. Goldberg, 1:400), rabbit anti-PfHsp70x (From J. Przyborski, 1:1000). The secondary antibodies that were used are IRDye 680CW goat anti-rabbit IgG and IRDye 800CW goat anti-mouse IgG (LICOR Biosciences, 1:20,000). The western blot images were processed and analyzed using the Odyssey infrared imaging system software (LICOR Biosciences).

Microscopy and image processing. For detection of HA-tags, PfHsp70x, PfFIKK4.2,

and MAHRP1, cells were smeared on a slide and acetone-fixed. For KAHRP detection, cells were fixed with paraformaldehyde (4%) and glutaraldehyde (0.075%). PfHsp70x-HA was detected using rat anti-HA antibody (clone 3F10, Roche, 1:100). MAHRP1 was detected using rabbit anti-MAHRP1 (from H-P Beck, 1:500). PfFIKK4.2 and KAHRP were detected using mouse anti-PfFIKK4.2 (1:1000) and mouse anti-KAHRP (1:1000 and 1:500, respectively. Both antibodies acquired from David Cavanagh, http://www.malariaresearch.eu/). Secondary antibodies used were anti rat-AlexaFluor 488 or 594, anti rabbit-AlexaFluor 488, and anti mouse-AlexaFluor 488 (Life Technologies, 1:100). Cells were mounted on ProLong Diamond with DAPI (Invitrogen) and were imaged using DeltaVision II microscope system with an Olympus IX-71 inverted microscope using a 100X objective. Image processing, analysis and display were preformed using SoftWorx and Adobe Photoshop. Adjustments to brightness and contrast were made for display purposes.

Acknowledgments

We thank Julie Nelson at the Center for Tropical and Emerging Global Diseases Cytometry Shared Resource Laboratory; Muthugapatti Kandasamy at the University of Georgia Biomedical Microscopy Core; Heather M. Bishop for technical assistance; Jose-Juan Lopez-Rubio for sharing the pUF1-Cas9 and pL6 plasmids; and Dan Goldberg (for anti-Plasmepsin V and anti-EF1α), Hans-Peter Beck (for anti-MAHRP), Jude Przyborski (for anti-PfHsp70x), and David Cavanagh and the European Malaria Reagent Repository (for anti-FIKK4.2 and anti-KAHRP). This work was supported by

grants from the March of Dimes Foundation (Basil O'Connor Starter Scholar Research Award), and the US National Institutes of Health (R00AI099156) to V.M.

References

1. WHO. World Malaria Report. World Health Organization. 2016.
2. Cowman AF, Healer J, Marapana D, Marsh K. Malaria□: Biology and Disease. Cell. 2015;167: 610–624. doi:10.1016/j.cell.2016.07.055
3. Nilsson SK, Childs LM, Buckee C, Marti M. Targeting Human Transmission Biology for Malaria Elimination. PLoS Pathog. 2015;11: e1004871. doi:10.1371/journal.ppat.1004871
4. Desai SA. Why do malaria parasites increase host erythrocyte permeability? Trends Parasitol. Elsevier Ltd; 2014;30: 151–159. doi:10.1016/j.pt.2014.01.003
5. Maier AG, Cooke BM, Cowman AF, Tilley L. Malaria parasite proteins that remodel the host erythrocyte. Nat Rev Microbiol. 2009;7: 341–354. doi:10.1038/nrmicro2110
6. Marti M, Good RT, Rug M, Knuepfer E, Cowman AF. Targeting Malaria Virulence and Remodeling Proteins to the Host Erythrocyte. Science. 2004;306: 1930–1933.
7. Hiller NL, Bhattacharjee S, Ooij C Van, Liolios K, Harrison T, Lopez-estran C, et al. A Host-Targeting Signal in Virulence Proteins Reveals a Secretome in Malarial Infection. Science. 2004;306: 1934–1937.
8. Klemba M, Goldberg DE. Characterization of plasmepsin V, a membrane-bound aspartic protease homolog in the endoplasmic reticulum of Plasmodium

falciparum. Mol Biochem Parasitol. 2005;143: 183–191. doi:10.1016/j.molbiopara.2005.05.015

9. Russo I, Babbitt S, Muralidharan V, Butler T, Oksman A, Goldberg DE. Plasmepsin V licenses Plasmodium proteins for export into the host erythrocyte. Nature. 2010;463: 632–6. doi:10.1038/nature08726

10. Boddey J a, Hodder AN, Günther S, Gilson PR, Patsiouras H, Kapp E a, et al. An aspartyl protease directs malaria effector proteins to the host cell. Nature. 2010;463: 627–631. doi:10.1038/nature08728

11. Haase S, Herrmann S, Grüring C, Heiber A, Jansen PW, Langer C, et al. Sequence requirements for the export of the Plasmodium falciparum Maurer's clefts protein REX2. Mol Microbiol. 2009;71: 1003–1017. doi:10.1111/j.1365-2958.2008.06582.x

12. Gruring C, Heiber A, Kruse F, Flemming S, Franci G, Colombo SF, et al. Uncovering common principles in protein export of malaria parasites. Cell Host Microbe. 2012;12: 717–729. doi:10.1016/j.chom.2012.09.010

13. de Koning-Ward TF, Gilson PR, Boddey JA, Rug M, Smith BJ, Papenfuss AT, et al. A newly discovered protein export machine in malaria parasites. Nature. 2009;459: 945–9. doi:10.1038/nature08104

14. Gehde N, Hinrichs C, Montilla I, Charpian S, Lingelbach K, Przyborski JM. Protein unfolding is an essential requirement for transport across the parasitophorous vacuolar membrane of Plasmodium falciparum. Mol Microbiol. 2009;71: 613–628. doi:10.1111/j.1365-2958.2008.06552.x

15. Riglar DT, Rogers KL, Hanssen E, Turnbull L, Bullen HE, Charnaud SC, et al.

Spatial association with PTEX complexes defines regions for effector export into Plasmodium falciparum-infected erythrocytes. Nat Commun. Nature Publishing Group; 2013;4: 1415. doi:10.1038/ncomms2449

16. Boddey JA. Inhibition of Plasmepsin V activity demonstrates its essential role in protein export, PfEMP1 display, and survival of malaria parasites. PLoS Biol. 2014;12: e1001897. doi:10.1371/journal.pbio.1001897

17. Hodder AN, Sleebs BE, Czabotar PE, Gazdik M, Xu Y, O'Neill MT, et al. Structural basis for plasmepsin V inhibition that blocks export of malaria proteins to human erythrocytes. Nat Struct Mol Biol. 2015;22: 590–596. doi:10.1038/nsmb.3061

18. Beck JR, Muralidharan V, Oksman A, Goldberg DE. PTEX component HSP101 mediates export of diverse malaria effectors into host erythrocytes. Nature. Nature Publishing Group; 2014;511: 592–5. doi:10.1038/nature13574

19. Elsworth B, Matthews K, Nie CQ, Kalanon M, Charnaud SC, Sanders PR, et al. PTEX is an essential nexus for protein export in malaria parasites. Nature. Nature Publishing Group; 2014;511: 587–91. doi:10.1038/nature13555

20. Maier AG, Rug M, O'Neill MT, Brown M, Chakravorty S, Szestak T, et al. Exported Proteins Required for Virulence and Rigidity of Plasmodium falciparum-Infected Human Erythrocytes. Cell. Elsevier Inc.; 2008;134: 48–61. doi:10.1016/j.cell.2008.04.051

21. Külzer S, Charnaud S, Dagan T, Riedel J, Mandal P, Pesce ER, et al. Plasmodium falciparum-encoded exported hsp70/hsp40 chaperone/co-chaperone complexes within the host erythrocyte. Cell Microbiol. 2012;14: 1784–1795.

doi:10.1111/j.1462-5822.2012.01840.x

22. Rhiel M, Bittl V, Tribensky A, Charnaud SC, Strecker M, Müller S, et al. Trafficking of the exported P. falciparum chaperone PfHsp70x. Sci Rep. 2016;6: 36174. doi:10.1038/srep36174

23. Mesen-Ramirez P, Reinsch F, Blancke Soares A, Bergmann B, Ullrich AK, Tenzer S, et al. Stable Translocation Intermediates Jam Global Protein Export in Plasmodium falciparum Parasites and Link the PTEX Component EXP2 with Translocation Activity. PLoS Pathog. 2016;12: 1–28. doi:10.1371/journal.ppat.1005618

24. Elsworth B, Sanders PR, Nebl T, Batinovic S, Kalanon M, Nie CQ, et al. Proteomic analysis reveals novel proteins associated with the Plasmodium protein exporter PTEX and a loss of complex stability upon truncation of the core PTEX component, PTEX150. Cell Microbiol. 2016; doi:10.1111/cmi.12596

25. Muralidharan V, Oksman A, Pal P, Lindquist S, Goldberg DE. Plasmodium falciparum heat shock protein 110 stabilizes the asparagine repeat-rich parasite proteome during malarial fevers. Nat Commun. Nature Publishing Group; 2012;3: 1310. doi:10.1038/ncomms2306

26. Prommana P, Uthaipibull C, Wongsombat C, Kamchonwongpaisan S, Yuthavong Y, Knuepfer E, et al. Inducible Knockdown of Plasmodium Gene Expression Using the glmS Ribozyme. PLoS One. 2013;8: 1–10. doi:10.1371/journal.pone.0073783

27. Muralidharan V, Oksman A, Iwamoto M, Wandless TJ, Goldberg DE. Asparagine repeat function in a Plasmodium falciparum protein assessed via a regulatable

fluorescent affinity tag. Proc Natl Acad Sci U S A. 2011;108: 4411–6. doi:10.1073/pnas.1018449108

28. Pei Y, Miller JL, Lindner SE, Vaughan AM, Torii M, Kappe SHI. Plasmodium yoelii inhibitor of cysteine proteases is exported to exomembrane structures and interacts with yoelipain-2 during asexual blood-stage development. Cell Microbiol. 2013;15: 1508–1526. doi:10.1111/cmi.12124

29. Nacer A, Claes A, Roberts A, Scheidig-Benatar C, Sakamoto H, Ghorbal M, et al. Discovery of a novel and conserved Plasmodium falciparum exported protein that is important for adhesion of PfEMP1 at the surface of infected erythrocytes. Cell Microbiol. 2015; doi:10.1111/cmi.12430

30. Ghorbal M, Gorman M, Macpherson CR, Martins RM, Scherf A, Lopez-Rubio J-J. Genome editing in the human malaria parasite Plasmodium falciparum using the CRISPR-Cas9 system. Nat Biotechnol. 2014;32: 819–21. doi:10.1038/nbt.2925

31. Kats LM, Fernandez KM, Glenister FK, Herrmann S, Buckingham DW, Siddiqui G, et al. An exported kinase (FIKK4.2) that mediates virulence-associated changes in Plasmodium falciparum-infected red blood cells. Int J Parasitol. Australian Society for Parasitology Inc.; 2014;44: 319–328. doi:10.1016/j.ijpara.2014.01.003

32. Watermeyer JM, Hale VL, Hackett F, Clare DK, Cutts EE, Vakonakis I, et al. A spiral scaffold underlies cytoadherent knobs in Plasmodium falciparum-infected erythrocytes. Blood. 2016;127: 343–51. doi:10.1182/blood-2015-10-674002

33. Spycher C, Rug M, Pachlatko E, Hanssen E, Ferguson D, Cowman AF, et al. The Maurer's cleft protein MAHRP1 is essential for trafficking of PfEMP1 to the surface of Plasmodium falciparum-infected erythrocytes. Mol Microbiol. 2008;68:

1300–1314. doi:10.1111/j.1365-2958.2008.06235.x

34. Pasini EME, Kirkegaard M, Mortensen P, Lutz HU, Thomas AW, Mann M. In-depth analysis of the membrane and cytosolic proteome of red blood cells. Blood. 2006;108: 791–801. doi:10.1182/blood-2005-11-007799.Supported

35. Banumathy G, Singh V, Tatu U. Host chaperones are recruited in membrane-bound complexes by Plasmodium falciparum. J Biol Chem. 2002;277: 3902–3912. doi:10.1074/jbc.M110513200

36. Egan ES, Jiang RHY, Moechtar MA, Barteneva NS, Weekes MP, Nobre L V, et al. A forward genetic screen identifies erythrocyte CD55 as essential for Plasmodium falciparum invasion. Science. 2015;348: 711–4. doi:10.1126/science.aaa3526

37. Drew ME, Banerjee R, Uffman EW, Gilbertson S, Rosenthal PJ, Goldberg DE. Plasmodium food vacuole plasmepsins are activated by falcipains. J Biol Chem. 2008;283: 12870–12876. doi:10.1074/jbc.M708949200

38. Russo I, Oksman A, Goldberg DE. Fatty acid acylation regulates trafficking of the unusual Plasmodium falciparum calpain to the nucleolus. Mol Microbiol. 2009;72: 229–245. doi:10.1111/j.1365-2958.2009.06639.x

39. Liu J, Gluzman IY, Drew ME, Goldberg DE. The role of Plasmodium falciparum food vacuole plasmepsins. J Biol Chem. 2005;280: 1432–1437. doi:10.1074/jbc.M409740200

40. Ganesan SM, Morrisey JM, Ke H, Painter HJ, Laroiya K, Phillips MA, et al. Yeast dihydroorotate dehydrogenase as a new selectable marker for Plasmodium falciparum transfection. Mol Biochem Parasitol. Elsevier B.V.; 2011;177: 29–34. doi:10.1016/j.molbiopara.2011.01.004

41. Klemba M, Gluzman I, Goldberg DE. A Plasmodium falciparum dipeptidyl aminopeptidase I participates in vacuolar hemoglobin degradation. J Biol Chem. 2004;279: 43000–43007. doi:10.1074/jbc.M408123200

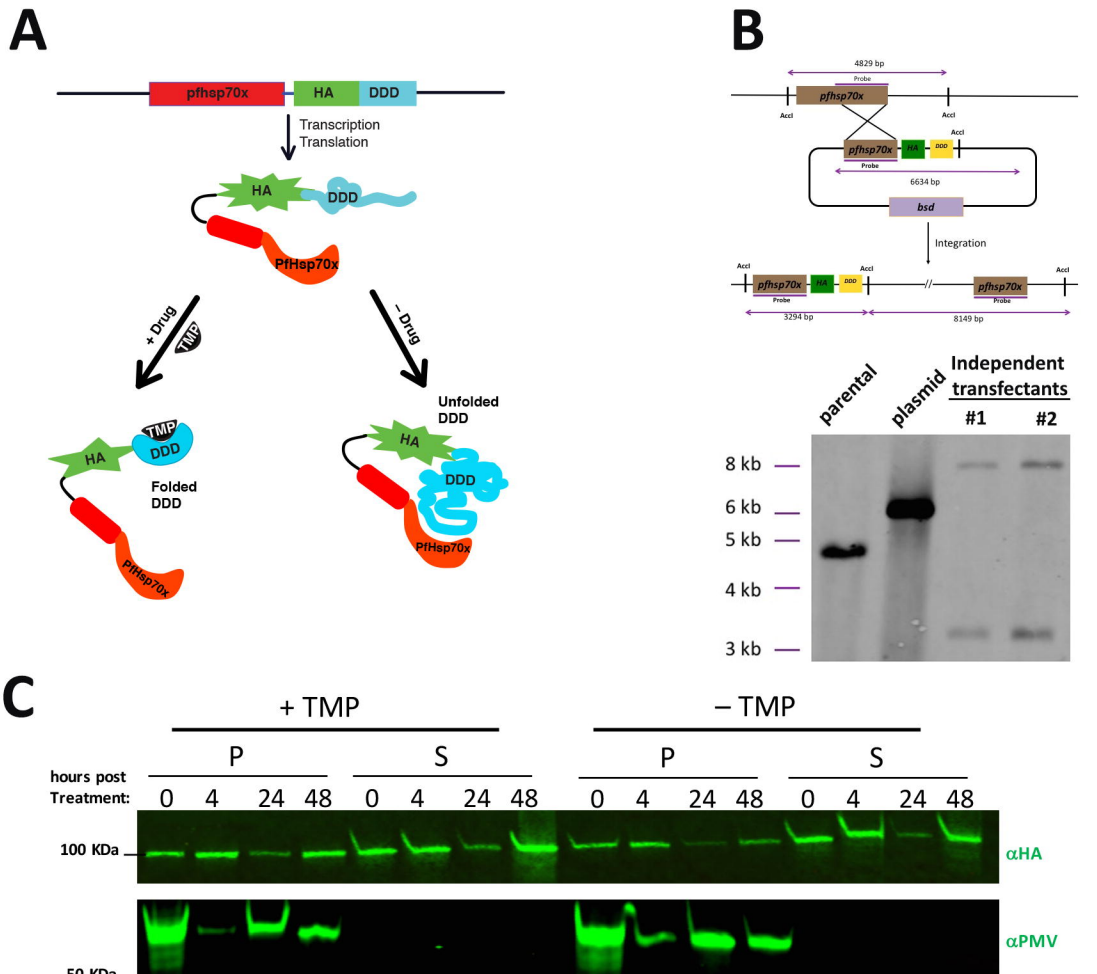
A
pfhsp70x
HA
DDD
Transcription
Translation
HA
DDD
PfHsp70x
+ Drug
TMP
– Drug
HA
TMP
DDD
Folded
DDD
PfHsp70x
Unfolded
DDD
HA
DDD
PfHsp70x
B
4829 bp
Probe
pfhsp70x
AccI
AccI
pfhsp70x
HA
DDD
AccI
Probe
6634 bp
bsd
Integration
AccI
pfhsp70x
HA
DDD
AccI
AccI
pfhsp70x
Probe
Probe
3294 bp
8149 bp
parental
plasmid
Independent
transfectants
#1
#2
8 kb
6 kb
5 kb
4 kb
3 kb
C
+ TMP
– TMP
P
S
P
S
hours post
Treatment:
0 4 24 48 0 4 24 48 0 4 24 48 0 4 24 48
100 KDa
αHA
αPMV
50 KDa

A

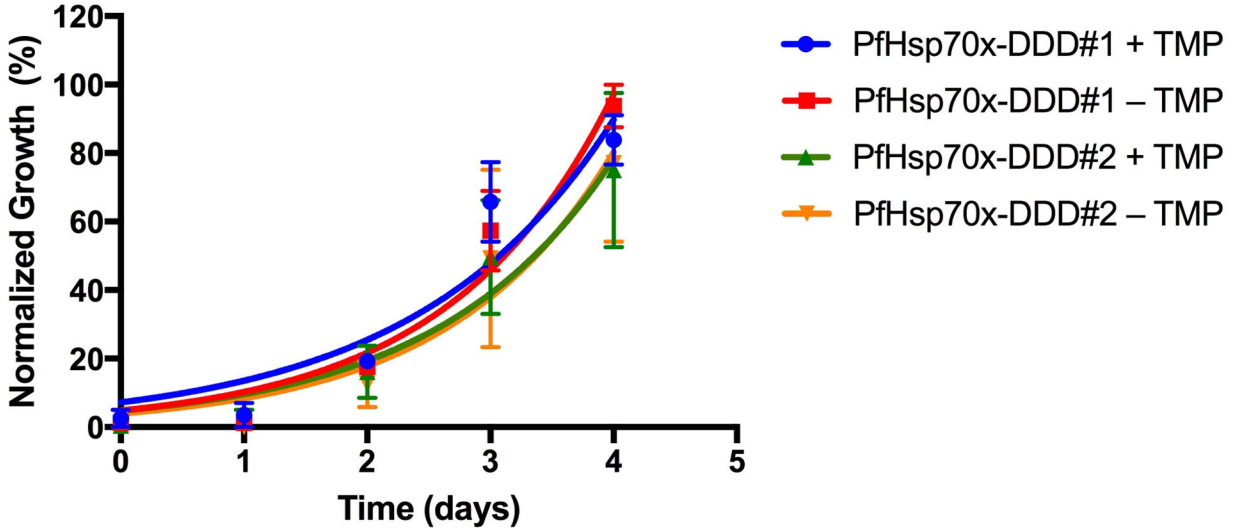
Normalized Growth (%)
120
100
80
60
40
20
0
0
1
2
3
4
5
Time (days)
PfHsp70x-DDD#1 + TMP
PfHsp70x-DDD#1 – TMP
PfHsp70x-DDD#2 + TMP
PfHsp70x-DDD#2 – TMP

B

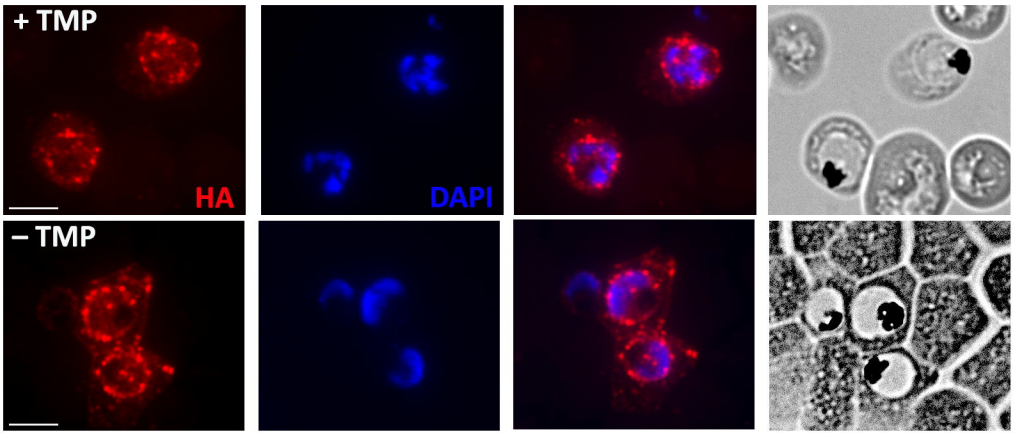
+ TMP
HA
DAPI
– TMP

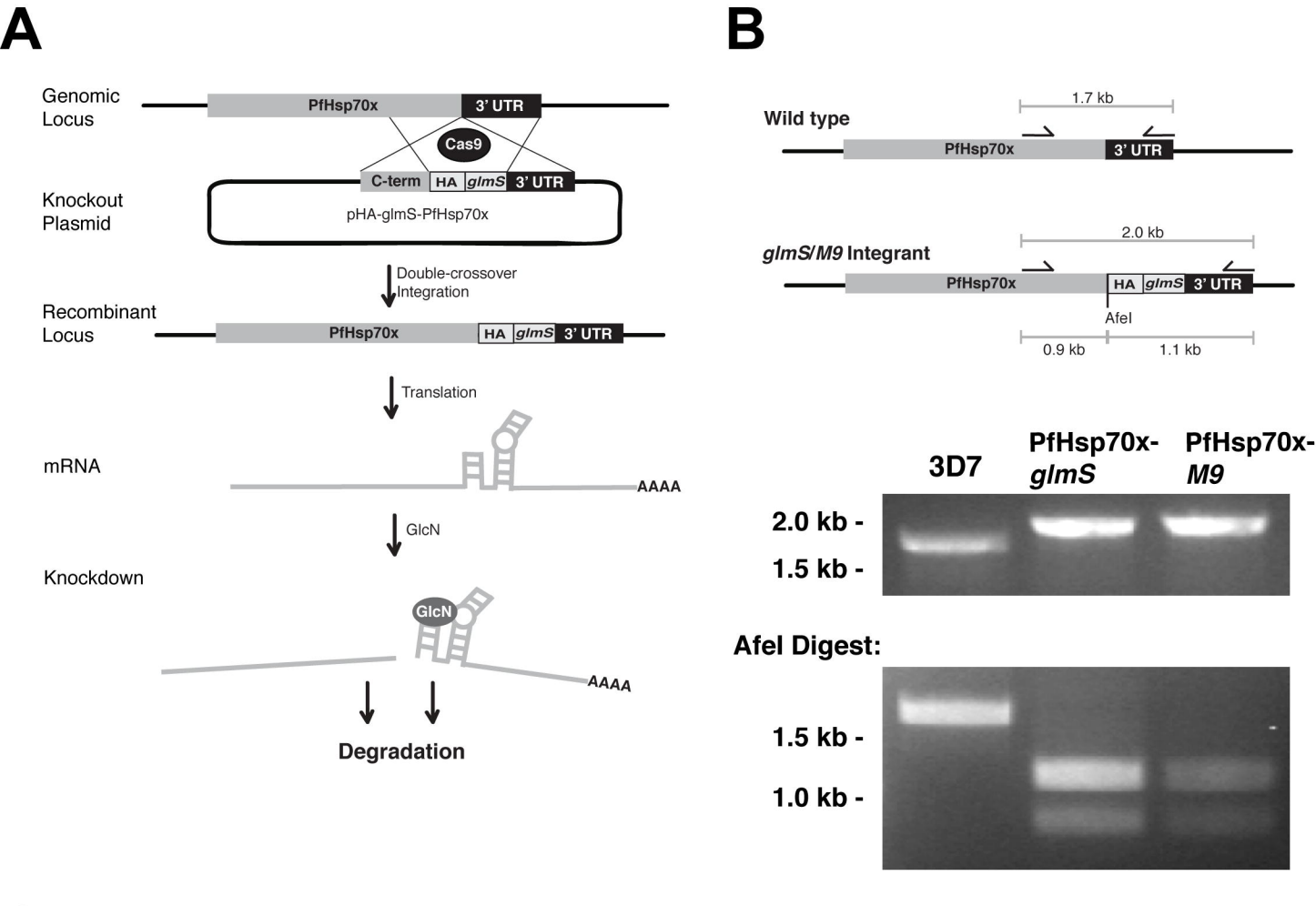
A
Genomic Locus
PfHsp70x
3' UTR
Cas9
C-term
HA
glmS
3' UTR
Knockout Plasmid
pHA-glmS-PfHsp70x
Double-crossover Integration
Recombinant Locus
PfHsp70x
HA
glmS
3' UTR
Translation
mRNA
AAAA
GlcN
Knockdown
GlcN
AAAA
Degradation
B
Wild type
1.7 kb
PfHsp70x
3' UTR
glmS/M9 Integrant
2.0 kb
PfHsp70x
HA
glmS
3' UTR
AfeI
0.9 kb
1.1 kb
3D7
PfHsp70x-glmS
PfHsp70x-M9
2.0 kb -
1.5 kb -
AfeI Digest:
1.5 kb -
1.0 kb -

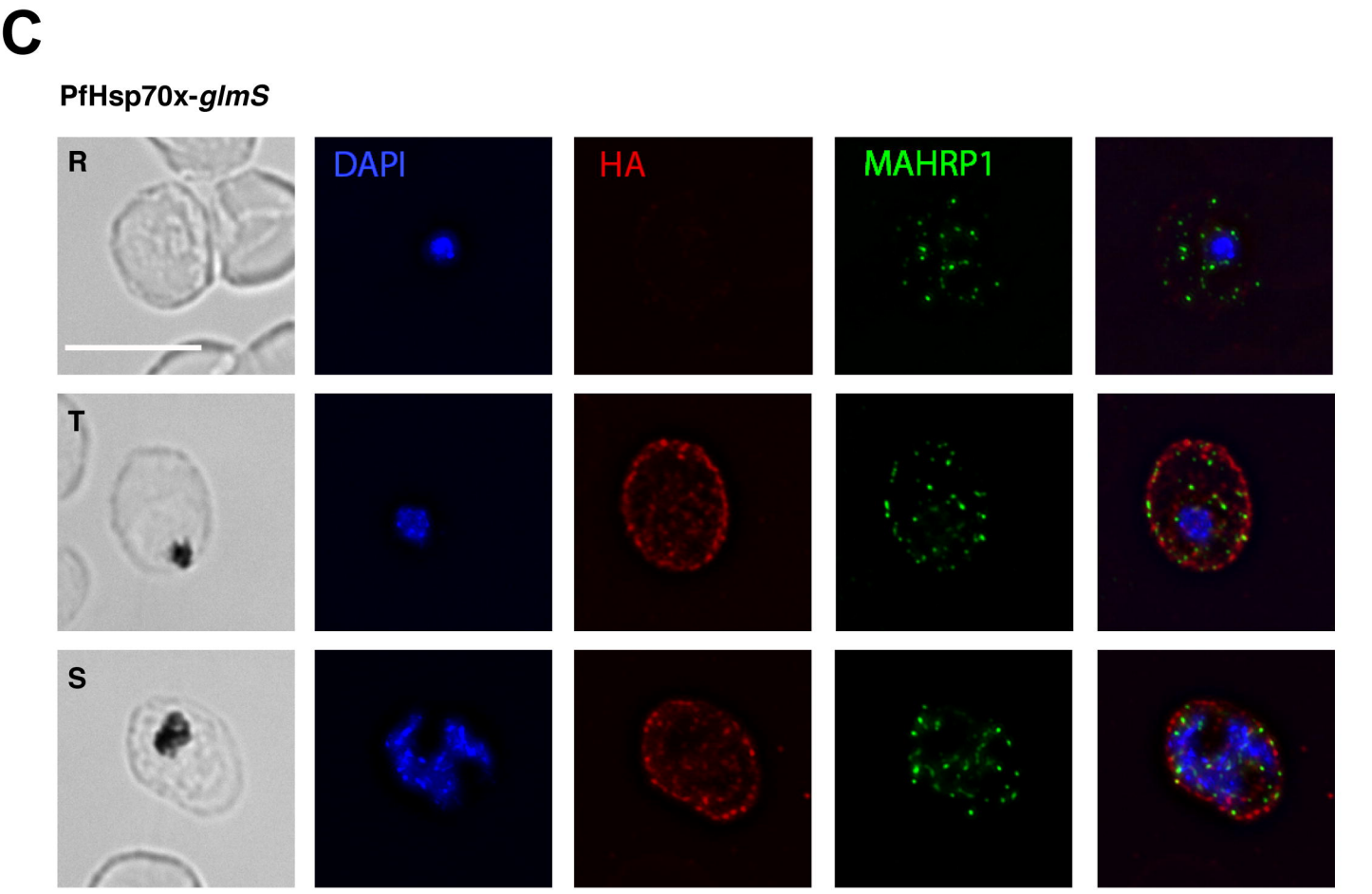
C
PfHsp70x-glmS
R
DAPI
HA
MAHRP1
T
S

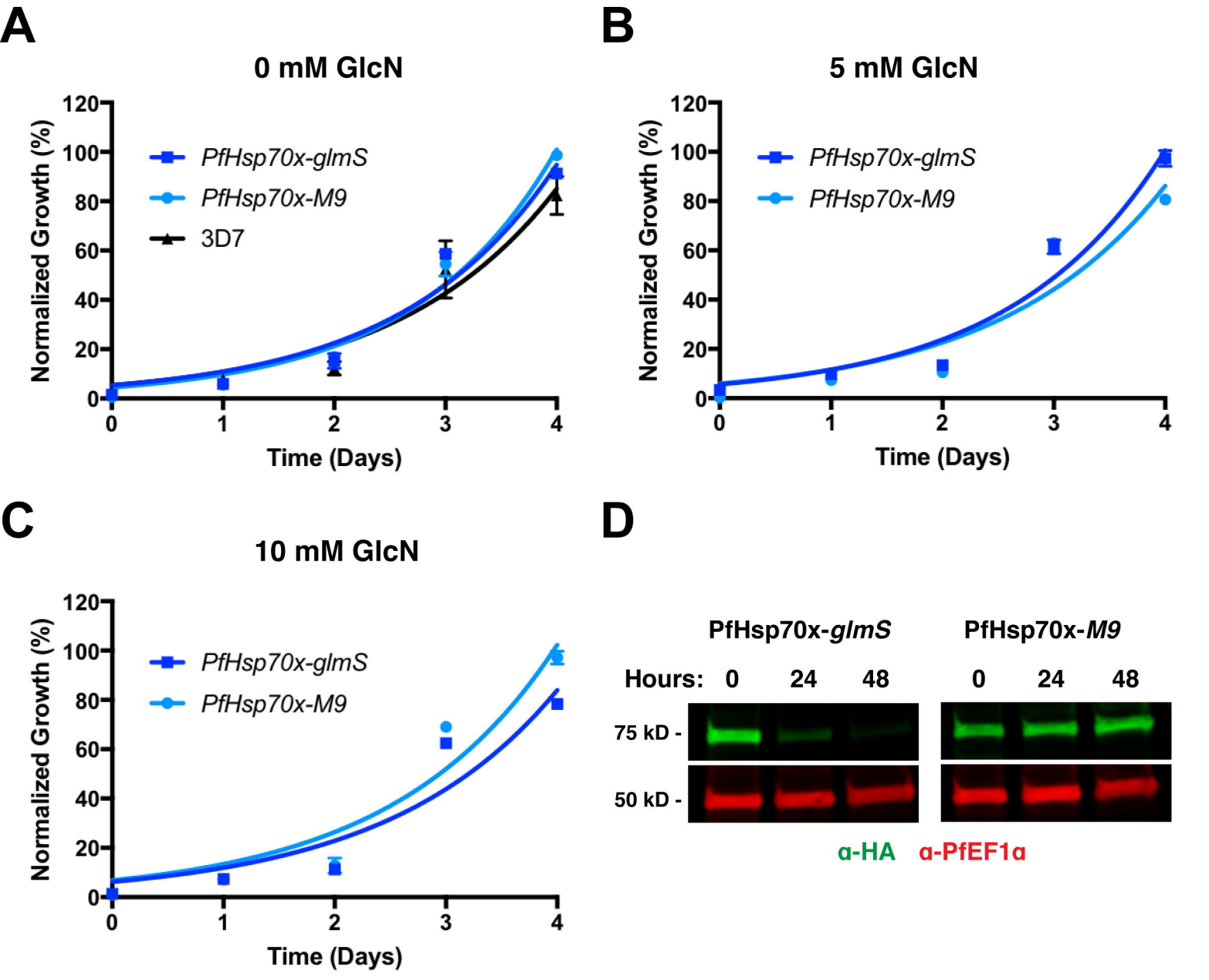
A
0 mM GlcN
Normalized Growth (%)
Time (Days)
PfHsp70x-glmS
PfHsp70x-M9
3D7
B
5 mM GlcN
Normalized Growth (%)
Time (Days)
PfHsp70x-glmS
PfHsp70x-M9
C
10 mM GlcN
Normalized Growth (%)
Time (Days)
PfHsp70x-glmS
PfHsp70x-M9
D
PfHsp70x-glmS
PfHsp70x-M9
Hours: 0 24 48 0 24 48
75 kD -
50 kD -
α-HA
α-PfEF1α

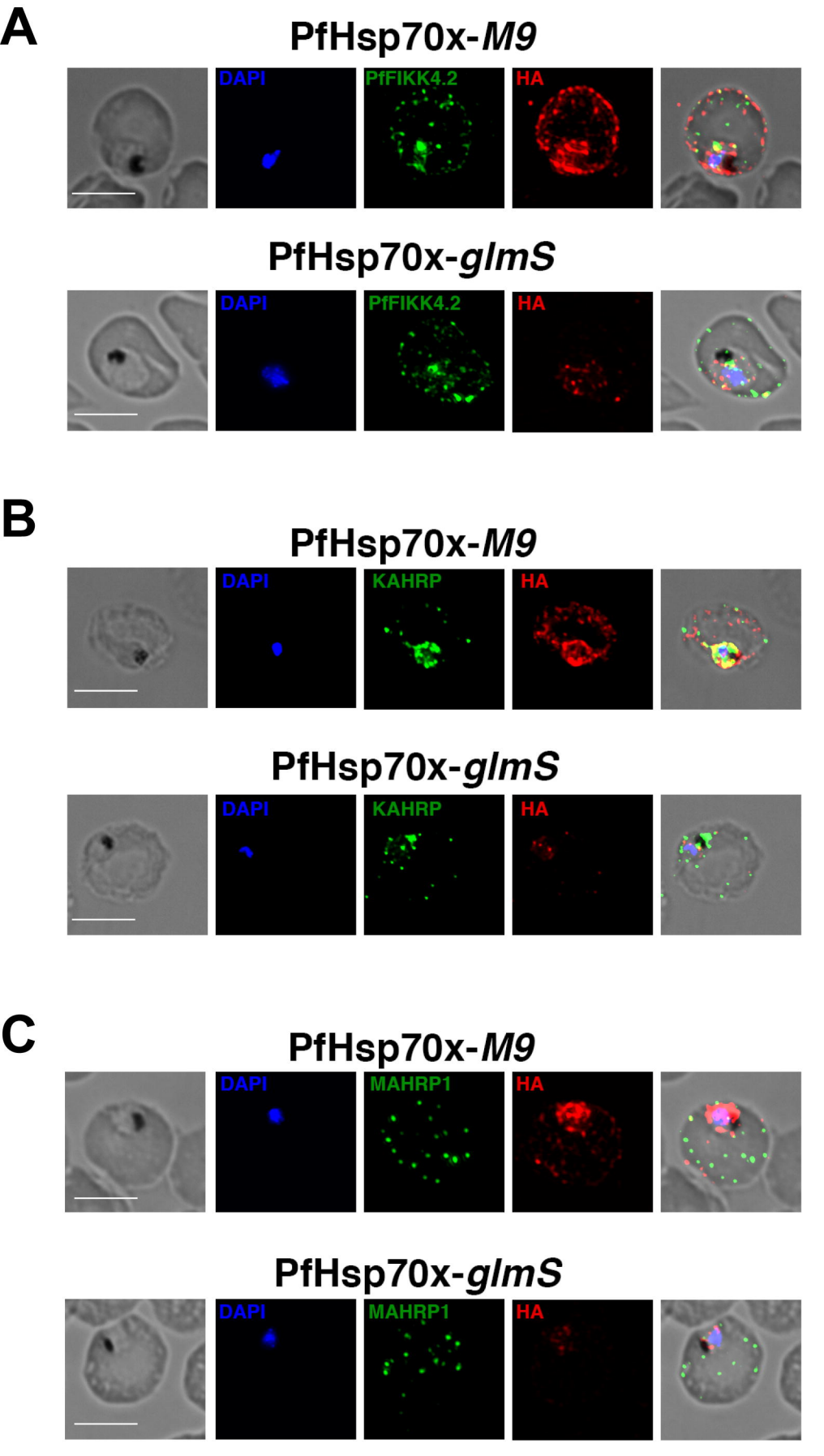
A
PfHsp70x-M9
DAPI
PfFIKK4.2
HA
PfHsp70x-glmS
DAPI
PfFIKK4.2
HA
B
PfHsp70x-M9
DAPI
KAHRP
HA
PfHsp70x-glmS
DAPI
KAHRP
HA
C
PfHsp70x-M9
DAPI
MAHRP1
HA
PfHsp70x-glmS
DAPI
MAHRP1
HA

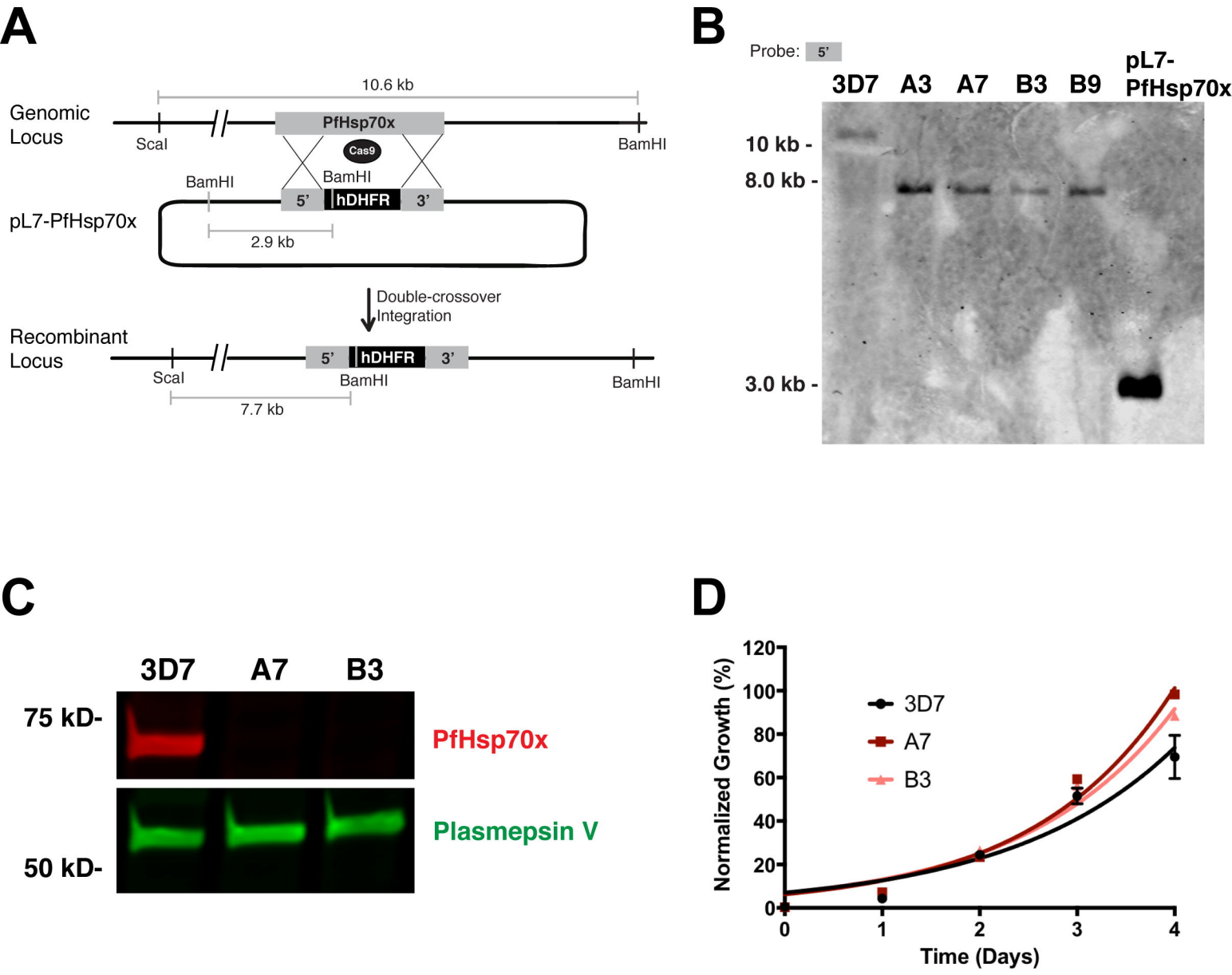
A
10.6 kb
Genomic Locus
ScaI
PfHsp70x
Cas9
BamHI
BamHI
BamHI
5'
hDHFR
3'
pL7-PfHsp70x
2.9 kb
Double-crossover Integration
Recombinant Locus
ScaI
5'
hDHFR
3'
BamHI
BamHI
7.7 kb
B
Probe: 5'
3D7
A3
A7
B3
B9
pL7-PfHsp70x
10 kb -
8.0 kb -
3.0 kb -
C
3D7
A7
B3
75 kD-
50 kD-
PfHsp70x
Plasmepsin V
D
Normalized Growth (%)
120
100
80
60
40
20
0
3D7
A7
B3
0
1
2
3
4
Time (Days)

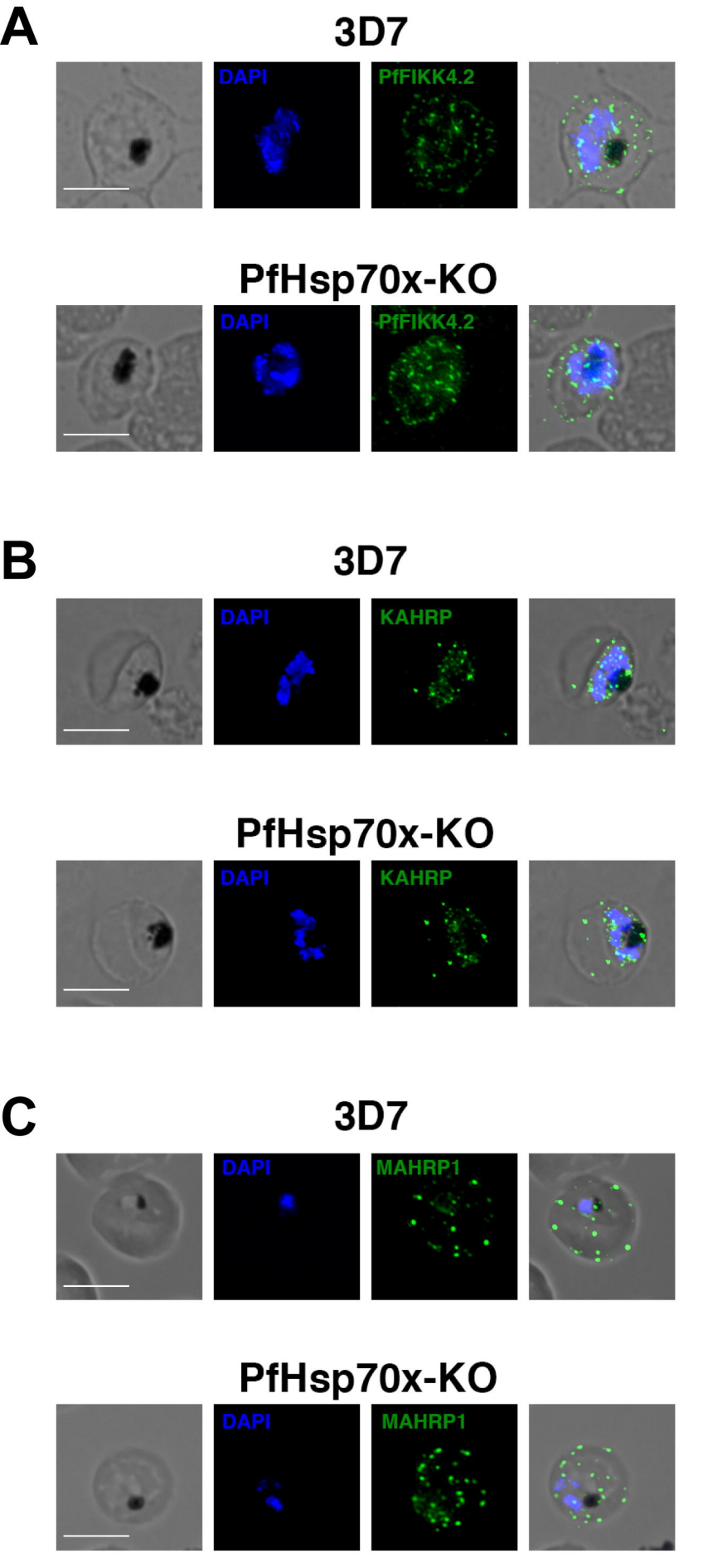
A
3D7
DAPI
PfFIKK4.2
PfHsp70x-KO
DAPI
PfFIKK4.2
B
3D7
DAPI
KAHRP
PfHsp70x-KO
DAPI
KAHRP
C
3D7
DAPI
MAHRP1
PfHsp70x-KO
DAPI
MAHRP1